JOURNAL OF MATERIALS SCIENCE 3 (1968) 306–313

The Dependence of Grain-Boundary Sliding on Shear Stress

R. C. GIFKINS
Baillieu Laboratory, The University, Melbourne, Victoria, Australia

A. GITTINS
Central Electricity Research Laboratories, Leatherhead, Surrey, UK

R. L. BELL
Engineering Laboratories, The University, Southampton, UK

T. G. LANGDON
Surface Physics, Cavendish Laboratory, The University, Cambridge, UK

Received 2 February 1968

Polycrystalline specimens of four materials: aluminium, a lead/thallium alloy, β-brass and Magnox AL80 were subjected to slow creep at a temperature of approximately 0.5 T_m (where T_m is the melting temperature in degrees Kelvin) and measurements made of the dependence of grain-boundary sliding on the orientation of the boundary with respect to the applied stress. The results were analysed in detail on the basis of the hypothesis that sliding is governed by the component of the applied stress resolved in the boundary plane. Agreement between theory and experiment leads to the conclusion that this is a most important factor governing sliding. The component of sliding revealed by steps on a free surface is seen to contain an extra term due to the unbalanced pressure from grains below the surface.

1. Introduction

In several recent studies of grain-boundary sliding the dependence of the extent of sliding on the angle θ made by a boundary trace with the stress axis has been examined [1-3]. The statistical significance of all of these results is open to question, and in at least one case [2] the specimen was only one grain thick, so that the situation was not representative of a true polycrystal. Nevertheless the results have been used to support the hypothesis that sliding is governed by the resolved shear stress acting on a boundary. An opposing view is that sliding merely accommodates the discontinuity in grain strain at the boundary and hence depends upon the resolved shear stress on the active slip planes [4, 5]. The present paper reports experiments on four different materials:— Aluminium, a lead/2% thallium alloy, β-brass, and Magnox AL80. Measurements of the dependence of sliding upon the orientation of the boundary trace with respect to the stress axis are compared with curves obtained on the hypothesis that sliding is governed by the component of the applied stress resolved in the boundary plane, and the agreement found suggests that this is the major factor controlling sliding. In the development of the theory several other detailed features of the results are satisfactorily explained.

2. Experimental Procedure

Four specimens were used for the measurements, one each of super purity aluminium, a lead/2% thallium alloy made from high purity elements, a 50:50 β-brass made from commercial grade copper and zinc, and Magnox AL80 (magnesium/0.78% aluminium alloy). All were obtained in the form of swaged or extruded rod. The shapes of the creep specimens varied, according to the dictates of the different creep machines employed,

but in all cases the cross-sections were such as to contain at least twenty-five grains across the smallest dimension. Before testing the specimens were annealed, polished either electrolytically or chemically, and marker lines both longitudinal and transverse to the axis were lightly scribed on the polished faces.

Creep was produced by dead loading at temperatures in the vicinity of 0.5 T_m, where T_m is the melting temperature in degrees Kelvin. After strains which extended well into the secondary stage of creep, the specimens were unloaded and measurements made of the three components of sliding (u, v and w see fig. 1) and the corresponding values of θ. On each specimen, at least 300 readings of each component were recorded.

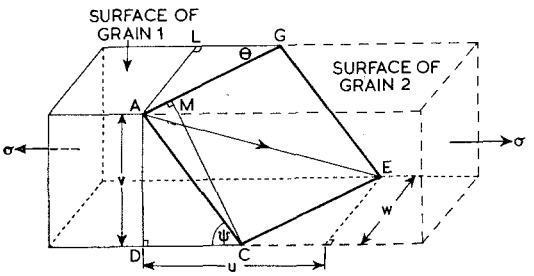

Figure 1 Diagram showing the components u, v and w due to the sliding of grain 2 over grain 1 at their mutual boundary AGEC. AE is the sliding vector.

Detailed accounts of the experimental procedures have been published elsewhere [6-8] but the essential characteristics of the specimens and testing conditions are given in table I.

3. Results

The measurements of the grain-boundary sliding components w and v are summarised in figs. 2 and 3. In these figures each point represents the average value of the measured sliding parameter for boundaries within a range of $\pm 5°$. The curves shown are not the best lines through

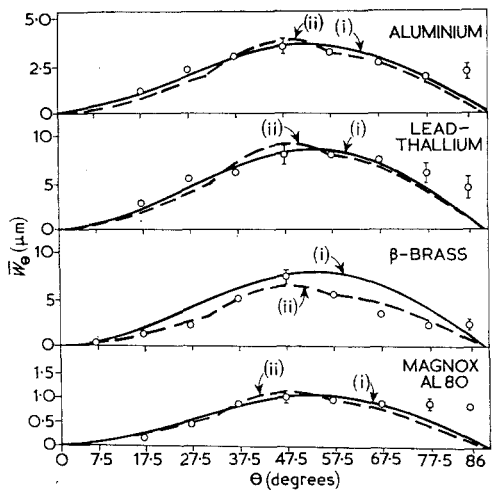

Figure 2 The dependence of the sliding component w on boundary angle θ. Open circles are experimental points; error bars represent the 95% confidence limits. Curves labelled (i) are theoretical curves, with sliding proportional to the first power of shear stress, matched with experiment at $\theta = 47.5°$. Curves labelled (ii) assume $n = 3$ at $32.5° < \theta < 57.5°$, and $n = 1$ outside these limits, matched with experiment at $\theta = 57.5°$.

experimental points but theoretical curves fitted at one point only, as will be explained later.

In all cases except one, the boundaries were sampled by working along longitudinal traverses of the specimen; the v-measurements for Magnox were made at randomly selected boundaries. Since a longitudinal traverse is more likely to intersect boundaries which are normal to it, the effect on figs. 2 and 3 of the longitudinal sampling procedure would be to give a higher accuracy at the larger θ-values where the averages were taken from greater numbers of readings. Averaging the w and v values over all θ's gave the results listed in table II. For each of the four specimens the values of w, fig. 2, rise from near zero at $\theta = 0$, to a maximum round about $\theta = 45°$, and fall again (but not to zero) as $\theta \to 90°$. The v-component, fig. 3, shows less

TABLE I Details of creep tests

Material	Grain size (μm)	Test temp. (° C)	Stress (psi*)	Duration of test (h)	Extension (%)
Super-pure aluminium	69	300	500	1030	19.5
Lead/2% thallium	180	21	600	2750	9.5
β-brass	360	420	450	8	9.6
Magnox AL80	100	200	2500	1000	2.5

*1.0 psi = 7.0×10^{-2} kg/cm²

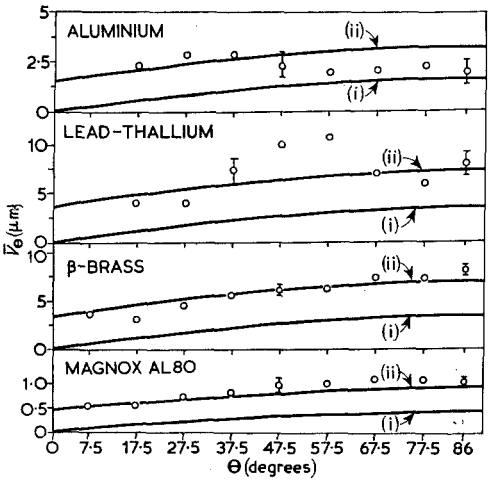

Figure 3 The dependence of the sliding component v on boundary angle θ. Open circles are experimental points; error bars represent the 95% confidence limits. Curves (i) are theoretical curves corresponding to (i) in fig. 2 and relying on the same matching point of $\theta = 47.5°$ used in that figure. Curves (ii) are obtained from (i) by the addition of $\bar{w}_{all\ \theta's}$ to each ordinate.

TABLE II Experimental and calculated values of $\bar{w}_l$ and $\bar{v}_l$

Material	$\bar{w}_l$, in μm		$\bar{v}_l$, in μm	
	Expt.	Theory	Expt.	Theory
Al	2.55	1.16	2.65	2.72
Pb/Tl	6.50	4.95	7.55	6.3
β-brass	4.50	4.70	6.80	5.94
Magnox	0.97	0.63	1.20	0.84

uniform behaviour, but two general tendencies are clear. Firstly, the smallest values of v (at $\theta \to 0°$) are a substantial fraction of the peak value of w for the same specimen; secondly, except in the case of the lead/thallium specimen, there is no pronounced maximum but rather an approximately linear dependence of v upon θ.

Values of u were measured and plotted, but are not reproduced here, since it can be shown [8-10] that u is a simple function of w and v.The shape of the u versus θ curves, although at first sight complex, merely confirmed this functional relationship between u, v, and w.

4. Theory

4.1. Assumptions and Procedure

The basic assumptions made are that grain-boundary sliding is governed by the component of the applied stress resolved in the boundary plane, and that its direction coincides with that of maximum shear stress in this plane. If the extent of sliding on the grain boundary AGEC in fig. 1 is represented by the vector AE then it is a consequence of our hypothesis that the components AC and CE will be determined by the shear stress in these two directions, and it is a simple matter to obtain the offsets v and w resulting from these components if θ and ψ are known.

Thus it is shown in Appendix 1 that

$$v = K(n) \sin \psi \left[\frac{\sigma \cos \psi}{(1 + \cot^2 \theta + \cot^2 \psi)^{\frac{1}{2}}}\right]^n \quad (1)$$

and

$$w = K(n) \sin \theta \left[\frac{\sigma \cos \theta}{(1 + \cot^2 \theta + \cot^2 \psi)^{\frac{1}{2}}}\right]^n \quad (2)$$

where σ is the applied tensile stress, and K is a constant (at a given instant in any one test) depending upon the value of the stress exponent n. In practice, the application of equations 1 and 2 is complicated by two factors. In the first place, the experimental results refer not to particular values of ψ, but rather to a range of ψ's for each measured value of θ. Individual values of ψ cannot be measured without sectioning, but the distribution functions at both "annealed" and "cut" surfaces are known, and so mean values of v and w may be calculated for each particular value of θ. Secondly, the construction of theoretical curves from these equations is clearly dependent on the choice of the stress exponent, n. These problems are discussed in detail in the following two sections.

4.2. Distribution functions for ψ

If a specimen is sectioned perpendicular to a freshly polished surface, it is found from measurements on the section that the probability of occurrence of boundaries making an angle ψ with the freshly polished surface is proportional to $\sin \psi$ [7, 8]. Now although this distribution function was in fact observed when boundaries of all θ's were counted, application of the Buffon needle theorem [11] suggests that it should apply equally where boundaries of any one θ value are concerned. Thus in the construction of w/θ and v/θ curves, suitable averages can be calculated by tabulating w (or v) for a series of values of ψ at each angle θ and applying a weighting proportional to $\sin \psi$ before taking the average.

In the case of an annealed surface or one on a specimen that has been subjected to prolonged high-temperature creep, the distribution of ψ is shifted to values approaching 90° [7, 8]. No simple function is found to describe these

results, but the empirically determined distribution is readily applied.

For a specimen that has been subjected to creep for only a short time the correct distribution function for ψ is somewhere between the two limits discussed above. The choice of a suitable average distribution function is dealt with in Appendix 2.

4.3. Stress Dependence

In any particular specimen the grain boundaries will experience shear stresses taking all values from half the applied tensile stress down to zero. This has an important bearing on the sliding because, just as the stress law for overall creep depends on the level of the stress, so has it been found recently in studies of grain-boundary sliding in bicrystals that the stress law for sliding also varies with the stress [12]. For lead the sliding rate is linear with the stress at shear stresses less than $\sim$150 psi (1.0 psi = 1.0 lb/in^2 = 7.0 $\times$ 10^{-2} kg/cm^2), but proportional to the cube of stress between $\sim$150 and $\sim$250 psi. The minimum creep rate of polycrystalline lead shows similar behaviour but with an additional 5 to 6 power-law stage at even higher stresses. Assuming the lead/thallium specimen used in the present experiments to show transitions at approximately the same stress levels, then with the applied tensile stress of 600 psi used in the present case, most of the boundaries would be subject to shear stresses in the linear range, and only those with θ near 45° and $\psi \rightarrow 90°$ would be in the cube-law region.

The stress exponent for creep in Magnox has been shown to increase from 1 to 7 with increase of stress [13] and in experiments carried out in conjunction with the present work the stress exponent for grain-boundary sliding was found to be 4.2 over the range of stresses from 2000 to 8000 psi at a test temperature of 200° C [8]. In view of the more detailed picture obtained for lead it seems likely that this value of 4.2 for Magnox represents an average of different values obtaining through the stress range. Since the experimental data used here refer to a tensile stress of only 2500 psi, values of $n = 3$ for θ near 45° and $n = 1$ for θ less than 30° or more than 60° seem appropriate.

For aluminium and β-brass there are no experimental results to give guidance on the stress dependence of n.

In the light of the above, two sets of theoretical curves were drawn. First $K(n = 1)$ was obtained by fitting at the peak experimental value of w. The theoretical curves constructed on this basis are labelled (i); these should give the best fit if $n = 1$ applied throughout. Second $K(n = 1)$ and $K(n = 3)$ were both obtained by fitting at $\theta = 57.5°$; the curves labelled (ii) were constructed using $K(n = 1)$ at θ less than 32.5° or greater than 57.5°, and $K(n = 3)$ at the intermediate angles. This procedure oversimplifies the situation, for it is not all boundaries with θ between 32.5° and 57.5° that are likely to have $K(n = 3)$, but only those for which ψ is close to 90°.

5. Comparison of Theory with Experiment

5.1. The w_θ versus θ Curves

Neglecting the experimental points at $\theta = 86°$ it is seen that the theoretical curve (ii), which was obtained using $n = 3$ at intermediate angles and $n = 1$ at the extremes, fits the data reasonably well for all four materials. For Magnox there is little to choose between the fit on the two theoretical curves, but with Pb/Tl and with Al the fit on curves (i) is even better than that on curves (ii). This makes good sense because in these cases the stresses were very low and one would expect the stress law with $n = 1$ to operate at almost all boundary angles.

The discrepancy which occurs at $\theta = 86°$ in all four cases may be due to one or two factors. Firstly if the direction of principal stress on any boundary is modified by the constraints of neighbouring grains, then at intermediate angles these deviations will cancel when averaged over a number of boundaries at a particular angle, but at $\theta \rightarrow 0°$ or $\theta \rightarrow 90°$ such deviations will only increase the sliding component, w. Because the resolved shear stress is much more sensitive to θ at angles approaching 90°, this effect is expected to be more pronounced at this extreme and, in fact, observed deviations from the theory were much greater at the high angle end than at the low. However, this may be only part of the story and a second important factor may be the extra freedom at boundaries meeting the surface at normal incidence.

5.2. The v_θ versus θ Curves

The curves labelled (i) in fig. 3 were drawn using values of $K(n = 1)$ obtained by matching theory and experiment at $\theta = 45°$ for w (in fig. 2). It is seen that these curves predict the correct trend for $\bar{v}_\theta$ versus θ but are displaced below the

experimental points by an approximately constant amount. The value of the addition to $\bar{v}_\theta$ which is required to cause approximate superimposition of the theoretical curve on to the experimental points turns out to be the mean value of $\bar{w}_\theta$ averaged over all θ's. We will call this $\bar{w}_{all\ \theta,s}$. The curves obtained using this addition are labelled (ii) in fig. 3.

A similar set of $\bar{v}_\theta$ curves transposed by additions of $\bar{w}_{all\ \theta,s}$ was obtained using $K(n = 3)$ and matching at 57.5° in fig. 2. These curves all fell below curves (ii) in fig. 3, so that (except perhaps for aluminium) there was considerably poorer fit than shown by curves (ii). Thus taking figs. 2 and 3 together, one is led to the conclusion that a stress law with $n = 1$ fits all the data best. This is reasonable if the critical stresses for changing from $n = 1$ to $n = 3$ are approximately half the applied tensile stresses used, for in that case not many boundaries, even with θ close to 45°, will have stresses sufficient to bring into operation the stress law with $n = 3$.

Having modified the theoretical $\bar{v}_\theta$ curves so as to produce reasonably good agreement with experiment, we must look for some physical justification for the procedure. This is obtained if we hypothesize that sliding perpendicular to the surface consists of two parts: (i) that due to the resolved component of the applied stress, and given by equation 1, and (ii) that due to the movement of the grains in the layers below the surface. In the interior of a polycrystal the grains are constrained equally on all sides and the components of sliding w and v are exactly equivalent, so that $\bar{w}_{all\ \theta,s} = \bar{v}_{all\ \theta,s}$. At the surface, however, movement in the v-direction lacks the constraint of grains beyond the surface, whereas movement in the w-direction is constrained in the same way as it is in the interior. Thus measurements of w made on the surface are found to give a reliable measure of w in the interior [14], and $\bar{w}_{all\ \theta,s}$ on the surface may be taken as equal to $\bar{v}_{all\ \theta,s}$ in the interior. The addition of $\bar{w}_{all\ \theta,s}$ thus represents the suggestion that the surface grains are pulled down by the underlying grains by an amount equal to their average displacement in the v-direction.

5.3. Values of $\bar{w}_l$ and $\bar{v}_l$

Experimental values for the averages of w and v obtained by summing all corresponding measurements along a longitudinal traverse are listed in table II. Since the v-measurements on Magnox referred to earlier were made on randomly selected boundaries, additional readings were taken along a longitudinal traverse to determine the average value quoted in table II. Theoretical values for $\bar{w}_l$ and $\bar{v}_l$ were obtained by averaging over all θ's in the theoretical curves of figs. 2 and 3, after first weighting the ordinate at each θ in proportion to $\sin\theta$, to take account of the probability of intersecting a boundary along a longitudinal traverse. Of the two theoretical curves for each of the different specimens in figs. 2 and 3, only the one giving the best fit with the experimental points was averaged in each case but it would make little difference had the averages been taken from the others. The agreement between theory and experiment is quite good for both w and v averages, but in each case there is a tendency for the theoretical values to be too small. This is the more marked in the case of w where the discrepancies between theoretical and experimental values of w_θ at $\theta \to 90°$ are very important in the calculation of $\bar{w}_l$, due to the $\sin\theta$ weighting.

5.4. Ratio $v_l/\bar{w}_l$

The ratio of v_l/w_l should depend upon the state of the surface of the specimen, ranging from a value of 1 for an annealed condition to a value of 2 for an as-cut condition. This is because $\bar{v}_l$ should equal $\bar{w}_l$ in the fully annealed condition, for with $\psi \to 90°$ the shear stress in the v-direction will be zero and the only contribution to $\bar{v}_l$ will be that imposed by the interior grains. In the as-cut condition $\bar{v}_l$ is made up from two components, each equal to $\bar{w}_l$.

In table II the ratios of $\bar{v}_l/\bar{w}_l$ are 1.1, 1.2, 1.5, and 1.2, confirming the assumption made that the average behaviour of these specimens is matched by supposing the attainment of an annealed condition to have dominated. Other specimens of these four materials gave similar ratios, but specimens of β-brass measured at low overall strains gave ratios between 1.7 and 1.9, showing the as-cut condition to be dominating at that stage. Results for twelve other specimens of β-brass [9] showed that the ratio was 1.5 ± 0.1 irrespective of grain size, stress (or rate of strain) provided that the strain were sufficiently large and that there were sufficient grains across the specimen thickness. This latter condition arises because the contribution to $\bar{v}_l$ from interior movement will drop to $\bar{w}_l/2$ when only three grains are present in the thickness of the specimen; it then follows that $\bar{v}_l/\bar{w}_l$ varies from 1.5 for an as-cut specimen to 0.5 for an annealed one.

A specimen of β-brass having three grains across its thickness in fact gave a ratio 0.78, which is about that to be expected if the rate of attainment of the annealed condition were similar to the twelve specimens mentioned above.

Repolishing specimens during creep will also increase the ratio $\bar{v}_l/\bar{w}_l$, but although experiments of this kind have been made [7-9], and increases indeed found, it has not been possible to predict the magnitude of the changes reliably. This is partly because of the difficulties of assessing the effects of the changes during creep from as-cut to annealed conditions; but it is also partly because of other structural changes which occur and which repolishing modifies [8].

6. Discussion

The previous section has shown that the theory based on a resolved shear stress criterion for grain-boundary sliding gives a good account of the general, and of many detailed, features of the observed behaviour. However, as expected, there are indications that the resolved component of the applied stress may be modified on a local scale by constraints due to neighbouring grains. In most cases these modifications cancel on averaging the observed behaviour over many grains, but in certain cases they do not. The most noteworthy exception occurs in the sliding component v measured at the surface. Here the unbalanced forces which arise from the movement of the interior grains give rise to a sliding term superimposed on that due to the resolved component of the applied stress.

The role of resolved shear stress in determining the rate of grain-boundary sliding favours rate-limiting mechanisms which involve the grain-boundary plane or one very close to it. The movement of dislocations in or near the boundary plane [15, 16] or the diffusion of protrusions along it [17] would each comply, but the motion of dislocations in the primary slip planes would not. The deduction by Rhines *et al* [4] concerning the importance of the resolved shear stress on the active slip planes might possibly be important if the accommodating slip at a grain boundary were limited to one or two principal slip planes. However, this does not seem to be a general limitation, for the accommodating slip in Pb-bicrystals was clearly seen on several systems unrelated to the criterion of maximum resolved shear stress [18]. The present results similarly lend no support for a related concept, put forward by Mullendore and Grant [5], that sliding represents the unresolved component of slip across a grain boundary. It may be that this condition can become overriding when the grain size becomes nearly equal to the specimen thickness, as was indeed the case in their experiments, but it is difficult to see how the present analysis could be successful if this were a general condition.

7. Conclusions

(i) The dependence of grain-boundary sliding on the orientation of the boundary with respect to the applied stress was measured for four different materials.
(ii) The experimental results were compared with theoretical curves calculated on the assumption that sliding was governed by the component of the applied stress resolved in the boundary plane.
(iii) Good agreement was found for the results obtained in the plane of the surface, but an additional term was necessary to account for sliding measured perpendicular to the surface.
(iv) It is concluded that, in general, grain-boundary sliding is dependent upon the resolved shear component of the applied stress, but that at the surface that component of sliding which is perpendicular to the surface is also influenced by the unbalanced forces arising from the movement of grains in the interior.

Acknowledgements

Various parts of this work were carried out in various places. Some of it (by T.G.L., R.L.B. and R.C.G.) at Imperial College, London in the School of Metallurgy, using facilities provided by Professor J. G. Ball and financed by the United Kingdom Atomic Energy Authority; some (by A.G.) during the tenure of a British Commonwealth Scholarship in the Metallurgy School, University of Melbourne with facilities provided by Professor H. W. Worner; and some (R.C.G.) formed part of the programme of research of the Physical Metallurgy Section of the Commonwealth Scientific and Industrial Research Organisation, and in this connexion thanks are due to Professor M. E. Hargreaves for his encouragement.

References

1. V. M. ROZENBERG and I. A. EPSHTEIN, *Fiz. Metall. i Metallov.* **9** (1960) 124.
2. J. G. HARPER, L. A. SHEPARD, and J. E. DORN, *Acta Met.* **6** (1958) 509.
3. S. L. COULING and C. S. ROBERTS, *Trans. AIME* **209** (1957) 1252.

4. F. N. RHINES, W. E. BOND, and M. A. KISSEL, *Trans. Amer Soc. Metals* **48** (1956) 919.
5. A. W. MULLENDORE and N. J. GRANT, *Trans. AIME* **227** (1963) 319.
6. R. C. GIFKINS, "Properties of Reactor Materials and Effects of Radiation Damage," edited by D. J. Littler (Butterworths, London, 1961).
7. A. GITTINS and R. C. GIFKINS, *Metal Sci. J.* **1** (1967) 15.
8. R. L. BELL and T. G. LANGDON, *J. Matls. Sci.* **2** (1967) 313.
9. A. GITTINS, Ph.D. thesis, University of Melbourne (1964).
10. R. N. STEVENS, *Metal. Reviews* **11** (1966) 129.
11. E. CZUBER, "Geometrische Wahrscheinlichkeiten und Mittelwerte" (B. G. Teubner, Leipzig, 1884) p. 84.
12. R. C. GIFKINS and K. U. SNOWDEN, *Trans. AIME* **239** (1967) 910.
13. J. E. HARRIS and R. B. JONES, CEGB Report No. RD/B/R144 (July, 1963).
14. C. GRAEME-BARBER, Ph.D. thesis, University of London (1967).
15. Y. ISHIDA and M. H. BROWN, *Acta. Met.* **15** (1967) 857.
16. R. C. GIFKINS, *Met. Sci. Eng.* **2** (1967) 181.
17. R. C. GIFKINS and K. U. SNOWDEN, *Nature* **212** (1966) 916.
18. P. R. STRUTT, A. M. LEWIS, and R. C. GIFKINS, *J. Inst. Metals* **93** (1964) 71.
19. R. A. SCRIVEN and H. D. WILLIAMS, *Trans. AIME* **233** (1965) 1593.

Appendix 1

Here expressions are derived for the components of grain-boundary sliding w and v in terms of the angles θ and ψ (fig. 1) using the assumptions detailed in the text. Scriven and Williams [19] treated the more general case when only values of θ are available; from the present experiments a good deal was known about the values of ψ and so a simple analysis is possible.

It follows from our assumptions that the rate of sliding in a particular direction x is given by

$$\frac{ds_x}{dt} = \frac{{\tau_x}^n}{\text{const.}} \qquad (1)$$

where τ_x is the resolved shear stress in the direction x and the stress exponent n has values of 1 or 3 depending on the level of stress. Providing n is invariant with time, it then follows by integration of equation 1 that the grain-boundary displacement after a time t_1 is given by

$$s_x = \frac{{\tau_x}^n}{\text{const.}}\, t_1 = K(n){\tau_x}^n \qquad (2)$$

Now suppose the column of specimen containing the grain boundary AGEC to sustain a tensile load P. The shear stress on this boundary in the direction AC will be

$$\frac{P\cos\psi}{\text{area AGEC}} = \frac{P\cos\psi}{\text{AG.MC}}$$

If the direction cosines of AG and AC are written down, it is then a straightforward matter to describe the angle $C\hat{A}G$ in terms of θ and ψ, and hence to obtain the product AG.MC, i.e. the area of AGEC. Thus the shear stress on the boundary is obtained as

$$\frac{P\cos\psi\sin\theta\sin\psi}{\text{AL.AD}\,(1-\cos^2\theta\cos^2\psi)^{\frac{1}{2}}} = \frac{\sigma\sin\theta\sin\psi\cos\psi}{(1-\cos^2\theta\cos^2\psi)^{\frac{1}{2}}}$$

where σ is the applied tensile stress.

Then substituting in equation 2 we obtain the displacement along AC after a time t_1 as

$$K(n)\left[\frac{\sigma\sin\theta\sin\psi\cos\psi}{(1-\cos^2\theta\cos^2\psi)^{\frac{1}{2}}}\right]^n$$

and the measurable offset v as

$$v = K(n)\left[\frac{\sigma\sin\theta\sin\psi\cos\psi}{(1-\cos^2\theta\cos^2\psi)^{\frac{1}{2}}}\right]^n \sin\psi$$

which may be simplified to

$$v = K(n)\sin\psi\left[\frac{\sigma\cos\psi}{(1+\cot^2\theta+\cot^2\psi)^{\frac{1}{2}}}\right]^n \qquad (3)$$

Similarly the offset w is obtained as

$$w = K(n)\left[\frac{\sigma\sin\theta\cos\theta\sin\psi}{(1-\cos^2\theta\cos^2\psi)^{\frac{1}{2}}}\right]^n \sin\theta$$

which may be simplified to

$$w = K(n)\sin\theta\left[\frac{\sigma\cos\theta}{(1+\cot^2\theta+\cot^2\psi)^{\frac{1}{2}}}\right]^n \qquad (4)$$

Appendix 2

This section gives details of the procedures used to calculate the theoretical $\bar{w}/\theta$ and $\bar{v}/\theta$ curves of figs. 2 and 3.

$\bar{w}/\theta$ Curves

Equation 4 was used to tabulate values of $w/K(n)$ with $n = 1$ for a series of values of ψ at a particular value of θ. Each value of $\bar{w}/K(1)$ so obtained was then weighted according to the appropriate distribution function for ψ before averaging to obtain $\bar{w}_\theta/K(1)$. The procedure was then repeated for different values of θ, and finally the whole set of computations repeated with $n = 3$.

Now we know from experiment that the distribution function for ψ changes during a creep test, from that typical of an as-cut surface at the beginning of a test to that corresponding to an annealed surface at some point during the test [7, 8]. To take account of this reorientation during the test two sets of values of $\bar{w}_\theta/K(n)$ were computed (for each value of n), and these were compounded by assuming that the as-cut configuration persisted for 30% of the duration of the test. This assumption is based on the observations on Magnox [8].

Values of $K(1)$ and $K(3)$ were obtained by substituting the experimental value of $\bar{w}$ at a particular value of θ (the choice of this matching point is discussed in section 4.3) and thus the whole of the theoretical curve could be constructed.

$\bar{v}/\theta$ Curves

The procedure here was very similar to that described above except that equation 3 was used in place of equation 4. Because of the similarity of the equations, a good deal of the labour in the tabulations of $v/K(n)$ was saved by interchanging θ and ψ in the tables prepared for $w/K(n)$. As before, weighting was applied to take account of the appropriate distribution function for ψ, and a compounded value obtained assuming the as-cut configuration to maintain for 30% of the time. In drawing the theoretical curves of v versus θ, the K values obtained by matching theory and experiment for w were used.